LA-UR-76-899

Contract 7405-E

TITLE: EXPLOSIVELY PRODUCED MEGAGAUSS FIELDS AND APPLICATIONS

MASTER

AUTHOR(S): C. M. Fowler, R. S. Caird, W. B. Garn and D. J. Erickson

SUBMITTED TO: Invited paper, Joint MMM-Intermag Conference, Pittsburg, PA, June 15-18, 1976. To be published in IEEE Transactions on Magnetics

los alamos
scientific laboratory
of the University of California
LOS ALAMOS, NEW MEXICO 87545

An Affirmative Action/Equal Opportunity Employer

Form No. 836
St. No. 2629
1/76

UNITED STATES
ENERGY RESEARCH AND
DEVELOPMENT ADMINISTRATION
CONTRACT W-7405-ENG. 36

EXPLOSIVELY PRODUCED MEGAGAUSS FIELDS AND APPLICATIONS*

C. M. Fowler, R. S. Caird, W. B. Garn and D. J. Erickson
Los Alamos Scientific Laboratory, University of California, Los Alamos, NM 87545

ABSTRACT

We describe various explosive magnetic flux compression devices that produce pulsed megagauss fields, and a number of applications in which they have been used. Among the systems described are relatively simple ones that generate fields up to 250 T in large fixed volumes, and cylindrical implosion systems that produce fields in excess of 1000 T. Small fixed volume systems are described that may be used in the laboratory. They require only small amounts of explosive and can produce 100 T fields in coils 25 mm long and 10 mm diameter. We discuss measurements made on various materials in megagauss fields, often at cryogenic temperatures, including magnetoresistance, magnetic susceptability, optical absorption, Faraday rotation, and Zeeman splittings. We also discuss experiments in which large magnetic pressures have been used to compress solid deuterium isentropically. In flux compression devices part of the energy of the explosives is converted to electromagnetic energy. This has led to their use as compact single-shot high power energy sources. At times, it is necessary to transformer couple loads to the device outputs. We describe successful operation of transformers in 165 T fields, and suggest that they can operate in much higher fields.

INTRODUCTION

Explosive flux compression devices are generally designed to produce very large magnetic fields or to generate large pulses of electromagnetic energy. The present discussion, as requested, surveys the high field program at the Los Alamos Scientific Laboratory, and therefore is limited largely to those devices that generate large magnetic fields in large working volumes and to the experiments that utilize these fields. We first describe several commonly used systems and present characteristic magnetic field versus time plots. Next described are high field diagnostics and experiments in which information is obtained electrically. This is followed by a description of several magneto-optical experiments. We then outline a series of experiments in which the large pressures accompanying high magnetic fields are used to compress solid deuterium isentropically to state conditions otherwise difficult to obtain. We conclude this discussion by

describing experiments in which transformers have been used successfully in pulsed high field environments greater than 100 T. This result is not entirely expected in view of the extreme effects of pressure and eddy current heating on conductors.

HIGH FIELD GENERATORS

Explosive flux compression devices consist basically of a cavity defined by surrounding metal conductors, some or all of which may be overlaid with explosives. After an initial magnetic flux is introduced in the cavity, the explosives are detonated. The subsequent motion of the conductors leads to compression of the flux into regions of smaller cross section or of lowered inductance. In analogy with engineering convention, such devices are called generators with their explosively driven components termed armatures. In some of these devices, magnetic flux is approximately conserved. Under this condition, both energy and current increase as the system inductance is forceably reduced by the moving conductors.

Schematic drawings of three flux compression generators are shown in Fig. 1. Other types of generators are described in references 1-4 and the references cited therein. Fig. 1a shows a cross sectional view of a strip generator. Initial flux is developed in the triangular generator cavity, bounded by copper sheet, and the cylindrical load coil, drilled out of a brass block. The flux is obtained from capacitor driven current supplied through the opening at the top left. Strips of sheet explosive, mounted on both plates of the generator, are detonated near peak system flux. Motion of the top strip first closes the current input slot, thus trapping the flux in the generator volume and load coil. As detonation proceeds along the strips the generator volume is reduced and the current and magnetic field increase in the system. The configuration of the copper plates during compression is shown by dashed lines at a time when the detonation fronts have progressed to the points labelled D. Peak fields developed depend on the load coil diameter and range from 100 T at 19 mm diam to 150 T for smaller diameters. Coil length variations, from 70 to 100 mm, have little effect on the peak fields developed. The magnetic field generated in a 16 mm diam load coil is shown in Fig. 2.

The amount of explosive used in this system varies from 0.75 to 1.50 kg. We are presently developing a miniaturized version of this generator for use in the laboratory. To date, fields of 110 T have been generated in load coils 25 mm long and 10 mm diam using less than 90 g of explosive. The generator body and

load coil are formed from a single sheet of copper 0.52 mm thick. A slotted piece of brass pipe is placed over the load coil to limit coil expansion from magnetic forces. The devices are not substantial enough for direct current feed. They are therefore placed within simply fabricated capacitor driven external coils that induce the required initial flux.

Fig. 1b shows a two-stage system. The first stage consists of a pair of strip generators. The second-stage cavity is the triangular wedge cut out of a brass block also containing the cylindrical load coil. The top plates of the strip generators and the plate over the second-stage cavity are formed from a single sheet of copper. The first-stage generators are driven by sheet explosive while the second-stage plate is driven by a block of pressed explosive initiated simultaneously over its surface. Initial flux is supplied to the complete system by capacitor driven current through the input opening at the upper left. At peak initial flux, the first-stage strip generator explosives are initiated. As detonation proceeds, flux is concentrated in the second-stage cavity. The second-stage initiation is timed to start compressing the flux in the triangular cavity at burnout of the strip generators. Peak fields obtained in the cylindrical load coils again depend upon the coil diameter. The higher field curve in Fig. 2 shows a field vs time plot obtained in a 16 mm diam coil. Peak fields of 175 T are typical for 19 mm diam coils, and about 250 T, for 10 mm diam coils.

Fig. 1c shows two axial views of a cylindrical implosion system. Initially, a thin walled metal cylinder or liner is centered within an annular charge of high explosive. Initial magnetic field B_0 is induced within the liner by energizing a pair of coils, one on each side of the liner, or a single coil large enough to house the entire assembly. A detonation system, such as the row of detonators shown, cylindrically initiates the explosive to start radial liner compression at peak initial flux. The right hand view in the figure shows the liner at a later stage of compression. Conservation of flux implies a magnetic field buildup inversely proportional to the square of the radius. However, field diffusion into the liner, lack of perfect implosion symmetry, and the large magnetic pressures developed limit the peak fields obtainable. Still, peak fields in the range 1000-1500 T were reported in the first flux compression experiments described in the literature.[5]

ELECTRICAL MEASUREMENTS

Electrical measurements in these systems pose special problems because of the rapid rates of magnetic

field rise. From Fig. 2, fields increase as fast as 10^7 T/s for the single-stage systems and still faster for the two-stage systems. In cylindrical implosion systems, rates larger than 10^9 T/s are normal during some phases of the implosion. Magnetic fields are usually determined by integrating the voltage signals obtained from small pickup coils of known area that are placed in the high field regions. It is especially necessary to guard against high voltage breakdown for implosion system measurements. Here probes with areas of only 10 mm^2 will develop potentials in excess of 10 kV. Care must also be taken to minimize stray areas that would contribute additional voltages to the probe signal. With use of twisted leads up to the active probe area, external shielding, and alignment of any necessary untwisted signal wires parallel to the field axis, our probes generally yield field measurements accurate to within 2% for the slow systems and 4% for the implosion systems. These measurements have been confirmed by measuring the Zeeman splittings of selected transitions and comparing the magnetic fields needed to calculate the observed splittings with fields determined from the probes.[6]

Great care in terms of technique is also necessary when accurate sample voltages are required to determine a physical quantity as a function of field. For example, we show in Fig. 3 the transverse magnetoresistance measured for Bi. The high field data was obtained using a single-stage strip generator. The sample was 4N polycrystalline Bi wire mounted transverse to the magnetic field. To permit longer sample lengths, a long rectangular load coil was machined into a brass block body, with about the same cross sectional area as a 19 mm diam cylindrical coil. The field pulse was therefore similar to that shown in Fig. 2, with a peak field of about 100 T. Current through the sample was monitored outside the high field volume and its measurement presented no difficulty. In contrast, the true voltage across the sample was obtained only after the measured voltage was corrected for pickup from the lead configuration. From Fig. 3, the magnetoresistance increases linearly to about 25 T with saturation beginning to appear at higher fields. In order to minimize Joule heating effects, current was passed through the sample for only 450 μs, the last 50 μs or so representing the time during which the shots were fired. Calculations showed that no appreciable rise in sample temperature took place under these conditions.

Another technique requiring special care is the measurement of the differential magnetic susceptibility in a rapidly changing magnetic field[7,8]. The basic technique employs two pickup loops of nearly equal areas with their planes normal to the field. One is

wound around the sample and gives a signal proportional to dH/dt + dM/dt. The second is located some distance from the sample and gives a signal proportional to dH/dt. Upon subtraction, the result is proportional to dM/dt. Dividing this by the signal proportional to dH/dt, one obtains the differential susceptibility dM/dH. The usefulness of the technique depends upon the accuracy in subtracting the two signals. The individual loop voltages are usually quite large and must be divided before monitoring. By making small adjustments in the division ratio for one of the loop signals small differences in coil areas can be compensated to yield an essentially null difference signal. These compensation tests are performed nondestructively on the assembly before the high field shot, using only capacitor bank discharges to supply the magnetic fields. With this procedure we have achieved a difference signal of less than 1% of the signal in either loop in sample free implosion experiments. This precision is sufficient to observe a first or second order magnetic transition in many materials. We plan to use this method to complement optical absorption techniques to determine the critical field for the spin flop to paramagnetic transition in MnF_2 as a function of temperature and orientation. We have previously presented optical data[9,10] that confirm theoretical predictions that this transition should occur at low temperature at about 1MG or twice the exchange field.

OPTICAL MEASUREMENTS

Our high field optical measurements have been confined primarily to the detection of visible light transmitted through various samples utilizing a high speed, rotating mirror spectrograph. This spectrographic camera covers, in a single shot, the complete visible spectrum over the high magnetic field range. Fig. 4 shows a schematic drawing of the system as adapted for a low temperature experiment. Intense light sources, which are reasonably white over most of the visible spectrum, are produced by shocking tubes of argon gas. The light is transmitted through the sample under investigation, passes through a grating that provides spectral resolution, impinges on a rotating mirror that provides time resolution, and finally is recorded on film. Magnetic fields are measured simultaneously by a pickup probe mounted in the annular space between the high field coil and the sample housing assembly. A bridgewire, mounted in the field of view of the spectrograph, is electrically exploded late in time of the experiment to produce a known spectrum on the film for wavelength calibration. With a standardized helium flow system, the samples

achieve temperatures of 6.5 ± 0.5 K at the time the experiments are initiated. Sample diameters are restricted to 6-7 mm for 200 T devices when the cryogenic housing is required.

We discuss here several representative experiments that are based on optical phenomena. Previous work is described elsewhere[9-12]. For example, Fig. 5 shows the transmission spectrum for thin platelets of GaSe obtained with the geometry shown in Fig. 4. The c axis of the crystal was aligned parallel to the magnetic field. The first several exciton absorption bands can be readily distinguished from the diffraction fringes visible at the longer wavelengths. From this record and several others derived from 200 T systems together with lower field data previously reported[10], we have tentatively adopted the level scheme shown in Fig. 6 for this material. Data obtained up to 17.5 T, shown in the rectangle at the lower left, were obtained by Aoyagi et al.[13] and by Halpern[14]. In Fig. 6, we have used the level notation of Aoyagi et al., with the exception of the very weak line previously unreported, labelled n = 1'. The other dashed lines indicate the existence of more than one absorption level, although owing to spectral resolution limitations, the locations are not very precise.

By mounting thin polaroid discs on both sides of the sample in Fig. 4, Faraday rotation experiments have been conducted. Fig. 7 shows a Faraday rotation record for a 1.02 mm long crystal of cubic phase ZnSe. The crystal was cut in such a way that the magnetic field was perpendicular to the {110} planes. The unusual character of the record can be understood by following a particular wavelength along the magnetic field. As the field increases, the polarization angle of the light increases. The light and dark regions then correspond to 90° rotation increments. The band reversals occur at peak magnetic field. Photodensitometer measurements across the record yield accurate positions of the peaks and valleys as functions of the field. Plots of the total angle of rotation vs magnetic field were straight lines for all wavelengths between 450 and 630 nm even though the clearly seen absorption band edge is around 440 nm. In contrast, similar experiments with CdS samples showed a marked curvature of the angles vs field for wavelengths near the absorption edge, particularly at the higher magnetic fields[10,12]. The resulting Verdet constants for ZnSe calculated from Fig. 7 are shown in Fig. 8.

We have also made high field Faraday rotation measurements with discrete wavelength lines, such as the green and blue lines of Hg. Photomultiplier tubes were used as the detectors, while pulsed mercury lamps with appropriate filters served as the sources. Al-

though this approach was abandoned in favor of the broadband method, we plan to initiate similar experiments with long wavelength laser sources. Besides Faraday rotation experiments, we intend to make infrared cyclotron resonance measurements similar to those of Herlach et al.[15] and Muira, Kido and Chikazumi[16].

As a last example, we describe briefly a series of Zeeman effect experiments. The spectra were displayed photographically as shown in Fig. 4. The light sources, however, were electrically exploded bridgewires placed in the high field region. In some cases, the bridgewires were coated lightly with other materials whose known spectra were desired. Although high field splittings were observed for many spectral lines, our primary motivation was to use the splittings of well understood lines as a means to calculate magnetic fields, thus furnishing a means of checking field values obtained from pickup probes as discussed above. The largest field measured in this manner was 510 T calculated from an observed 16.5 nm splitting of the Na D lines[6].

MAGNETIC FIELDS AS PRESSURE SOURCES

Fig. 9 is a schematic of an experiment used to obtain high pressure equation of state data for solid deuterium. The experiments are being done jointly with members of our laboratory cryogenics group, who designed the sample holders and furnish the deuterium loaded samples at shot time. The outer vacuum wall of the sample holder is nonconducting, while the inner wall is copper. The entire sample assembly fits into a 16 mm diam load coil. The high field system employed is the two-stage system of Fig. 1b. As the field builds up in the annular space between the field coil and the deuterium confining copper sleeve, the magnetic pressure compresses the sleeve, and consequently, the deuterium sample. The primary diagnostics consist of a field probe, which monitors the field during the entire compression stage, and a 600 kV flash x-ray pulse, aligned to radiograph the cross section of the deuterium sample. Limited to a single x-ray exposure during a shot, the pulse is timed to correspond to a particular magnetic field during the compression stage.

Fig. 10 shows an x-ray exposure of the setup configuration, and an exposure taken during the implosion phase when the field was 128 T. From the right ordinate of Fig. 2, the drive pressure for this field is 6.5 GPa (65 kb). With use of image quantizing equipment, the areal compression of the deuterium determined from the radiographs was 3.55 ± 0.50, leading to a tentative state (p,ρ) point of (6.5 GPa, 0.71 ± 0.10 g/cm3).

The interpretation and validity of the data rest heavily on calculational results. A number of one dimensional hydrodynamic calculations were made to investigate the uniformity of the deuterium sample over the cross section, using hypothetical deuterium equations of state and copper sleeve drive pressures corresponding to the field curve of Fig. 2. The calculations showed that for the last several microseconds of compression, the pressures and densities over the deuterium cross section were quite uniform, and further, that the deuterium pressure was the same as that of the magnetic drive pressure to within a few percent. A second result from these calculations was that the compression was essentially isentropic. This contrasts sharply with shock compression to the same pressure where, for compressible materials, significant increases in entropy and far greater temperatures are obtained with substantially less compression. A few two dimensional hydrodynamic calculations were done, again using hypothetical models for the deuterium equation of state. Results from these calculations showed that there was also negligible axial variation of density and pressure in the central region of the sample. This is the region of greatest compression and defines the sample cross sections shown in the radiographs.

Two lower pressure data points have also been obtained, the lowest of which agrees within our experimental error with that of Stewart[17]. All data points are assumed to belong to the isentrope passing through the initial conditions of the experiment (ρ_o = 0.200 g/cm^3, T_o = 10K).

So far, we have been limited in pressure to about 6.5 GPa, because of x-ray beam attenuation at the higher deuterium densities. A more energetic 2 MeV machine has recently become available, which should permit an extension of the data to 15 GPa, probably with better volume resolution, and therefore greater density accuracy.

Although our present data are not very precise, the method seems particularly suited for high pressure equation of state investigations of soft materials at low temperatures. As noted above, the use of fixed volume load coils allows measurement of both pressure and volume, along an isentropic thermodynamic path. Much higher pressures can be obtained with implosion systems, such as shown in Fig. 1c. The pressures, however, cannot be monitored during the final stages of compression, because the field measuring probes are destroyed. For this reason, when implosion systems have been used in compression experiments, the pressures have had to be inferred, such as in our early imploding liner plasma compression experiments[18], or in the more recent work by Hawke and coworkers[19] in their attempts to make metallic hydrogen. More accurate high

pressure data have been obtained by shock techniques, but since the thermodynamic paths are such that the data points are far removed from those obtained isentropically, the two techniques are complementary. Low temperature isothermal data can also be obtained in hydrostatic presses, but accurate (p,ρ) data for deuterium have been limited to only a few GPa[17,20].

HIGH FIELD ENVIRONMENTS

The current densities required to produce large fields lead to destructive effects upon metal conductors. Furth, Waniek and Levine[21], in a classic paper, have considered both pressure and temperature effects. Using a simplified analysis, they concluded that the surface temperature of several different metals placed in a magnetic field B rose approximately as $\Delta T(K) = 0.3 B^2$. They then characterized these metals by a critical field above which melting would begin. The fields generally ranged from about 50 T for copper to about 100 T for tungsten. The analysis showed that the coefficient 0.3 was pulse shape dependent, but not time dependent. Later, more detailed work[22] has shown that the interaction of a large field with a metal is far more complicated and is time dependent. Generally, larger magnetic fields can be produced when pulse times are shorter, such as the 1000 T and greater fields produced in cylindrical implosion systems. Here, it is almost certain that the inner surface of the liner has melted and has perhaps even achieved a plasma state.

Knowing that the actively driven liners were able to function under these extreme conditions, it was by no means certain that a passive element, such as a transformer, could survive in a high field environment. To investigate this point, a number of experiments were performed in which small, multiturn transformers were placed in high field load coils. The first attempts resulted in failure usually caused by turn-to-turn coil breakdown before peak fields were reached. It should be noted that a shorting of a turn in these pulsed systems effectively excludes further flux from penetrating the windings, thus terminating the transformer action. The breakdown problem was eliminated by winding the coils on a soft substrate, such as polyethylene. Apparently, softer materials are able to adapt as the transformer windings distort such that turn-to-turn insulation is preserved. With primary coils driven by single-stage flux compression systems (Fig. 1a), transformers were shown to function properly in peak fields as large as 110 T. Fig. 2 shows that the field rise time is about 7 μs (from 0.5 max to max). With a two-stage system (Fig. 1b), successful transformer operation was achieved in fields of 165 T with field rise

times of 4-5 microseconds. Based upon these results, we now have some confidence that transformers should function in implosion produced fields of 500-1000 T, where the rise times are less than one microsecond.

The importance of these transformer studies is associated with the use of transformers in flux compression devices that are used as power sources. Such devices are inherently low impedance sources, and are best suited for driving low inductance loads. The transformers serve as impedance matching transfer systems enabling us to power widely differing loads including resistive elements, large inductors, and capacitors. Often the primary load coils can be made large enough that the resulting fields are sufficiently low to prevent serious damage to the transformers. However, there remain situations where small coils may be required for compactness or for very fast energetic pulses that can be obtained only by the ultra high fields produced by implosion systems.

ACKNOWLEDGEMENTS

We are indebted to many Los Alamos people who have contributed to various parts of this program, in particular to D. B. Thomson who worked with us for a number of years. Our collaborators on the deuterium compression experiments are R. Mills and F. Edeskuty from the laboratory cryogenics group, and we have received calculational and theoretical support on this program from J. N. Fritz, G. I. Kerley, and S. R. Orr. We are also indebted to W. G. Witteman who grew the GaSe crystals used in the optical transmission experiments.

REFERENCES

* Work done under the auspices of the United States Energy Research and Development Administration.

1. Proceedings of the Conference on Megagauss Magnetic Field Generation by Explosives and Related Experiments, H. Knoepfel and F. Herlach, Eds. (Euratom, Brussels, 1966).
2. F. Herlach, Rept. Prog. Phys. 31, 341 (1968).
3. H. Knoepfel, Pulsed High Magnetic Fields (North-Holland, Amsterdam, 1970).
4. C. M. Fowler, R. S. Caird, and W. B. Garn, Los Alamos Scientific Laboratory report LA-5890-MS (1975).
5. C. M. Fowler, W. B. Garn, and R. S. Caird, J. Appl. Phys. 31, 588 (1960).
6. W. B. Garn, R. S. Caird, D. B. Thomson, and C. M. Fowler, Rev. Sci. Instr. 37, 762 (1966).
7. S. Foner and S.-L. Hou, J. Appl. Phys. 33 (Suppl.), 1289 (1962).

8. K. W. Blazer and H. Rohrer, Phys. Rev. 173, 574 (1968).
9. R. S. Caird, W. B. Garn, C. M. Fowler, and D. B. Thomson, J. Appl. Phys. 42, 1651 (1971).
10. C. M. Fowler, Science 180, 261 (1973).
11. W. B. Garn, R. S. Caird, C. M. Fowler, and D. B. Thomson, Rev. Sci. Instr. 39, 1313 (1968).
12. R. S. Caird, C. M. Fowler, J. N. Fritz, W. B. Garn, and D. B. Thomson, Los Alamos Scientific Laboratory report LA-5065-MS (1972).
13. K. Aoyagi, A. Misu, G. Kuwabara, Y. Nishina, S. Kurita, T. Fukuroi, O. Akimoto, H. Hasegawa, M. Shinada, and S. Sugano, J. Phys. Soc. Jap. 21 (Suppl.), 174 (1966).
14. J. Halpern, J. Phys. Soc. Jap. 21 (Suppl.), 180 (1966).
15. F. Herlach, J. Davis, R. Schmidt, and H. Spector, Phys. Rev. B10, 682 (1974).
16. N. Miura, G. Kido, and S. Chikazumi, Univ. of Tokyo ISSP report No. 723-Ser. A (1975).
17. J. W. Stewart, J. Phys. Chem. Solids 1, 146 (1956).
18. "Atomic Energy Research in the Life and Physical Sciences" (report of the U. S. Atomic Energy Commission, available from the Superintendent of Documents, Government Printing Office, Washington D. C., 1960), p. 104; see also D. B. Thomson, R. S. Caird, W. B. Garn, and C. M. Fowler, in Ref. 1, p. 491.
19. R. Hawke, D. Duerre, J. Huebel, R. Keeler and H. Klapper, Phys. Earth Planet. Inter. 6, 44 (1972).
20. M. S. Anderson and C. A. Swenson, Phys. Rev. B10, 5184 (1974).
21. H. P. Furth, M. A. Levine, and R. W. Waniek, Rev. Sci. Instr. 28, 949 (1957).
22. R. E. Kidder, in Ref. 1, p. 37.

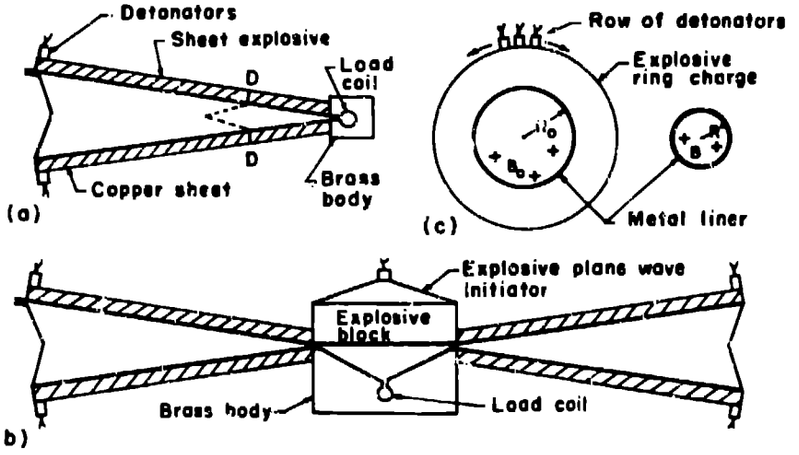

Fig. 1. Cross-sectional views of three high field flux compression devices, (a) single-stage strip system, typical peak field is 110 T in 16 mm diam load coil; (b) two-stage system, typical peak field is 200 T in 16 mm diam load coil; (c) cylindrical implosion system, peak fields exceed 1000 T in diameter of a few mm.

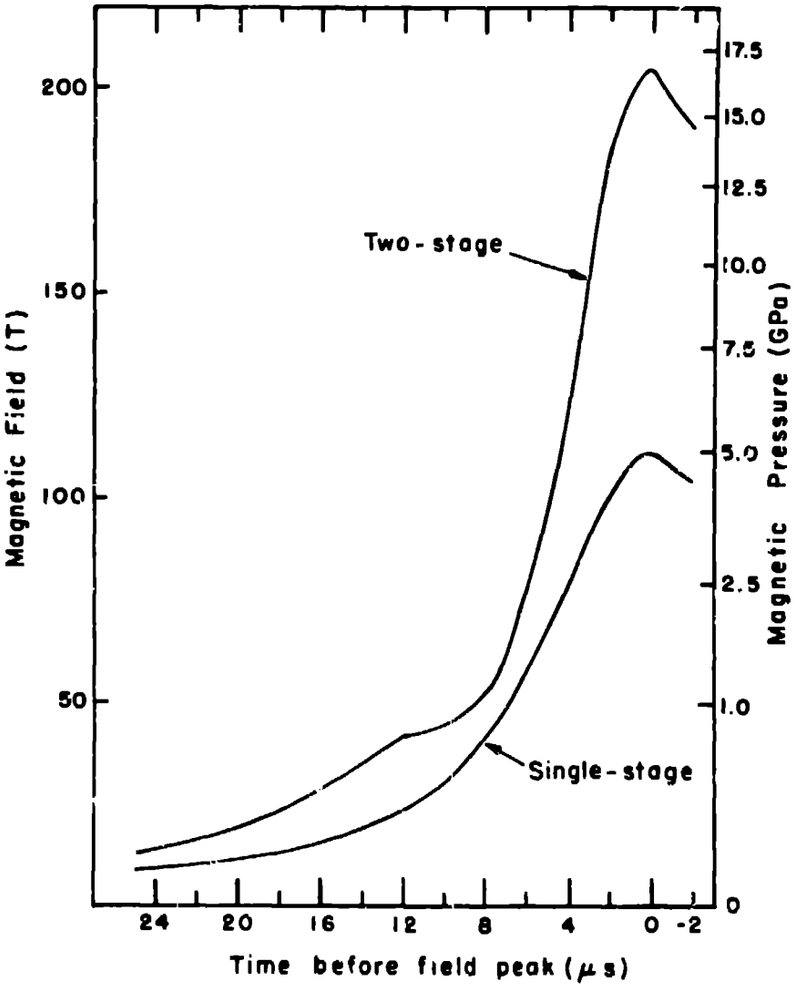

Fig. 2. Magnetic field and corresponding magnetic pressure developed in 16 mm diam load coils vs time for the single-stage and two-stage systems.

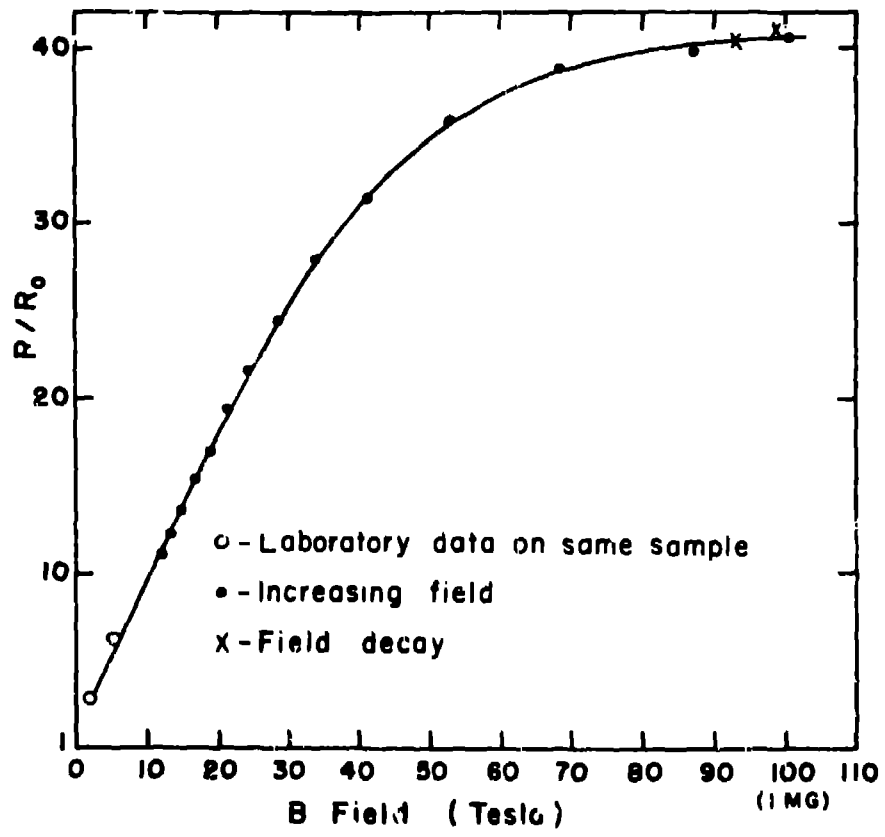

Fig. 3. The normalized transverse magnetoresistance of Bi at about 300 K. Open circles represent data obtained nondestructively in the laboratory. The data represented by X's were obtained during the decay of the field after peak was reached. All other data were taken while the field was increasing.

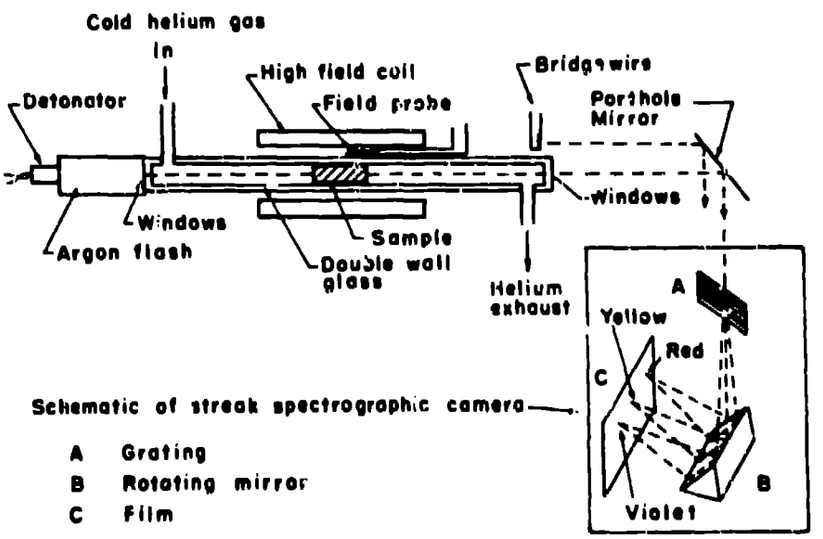

Fig. 4. Schematic diagram of a setup used for low temperature, high field, optical transmission experiments.

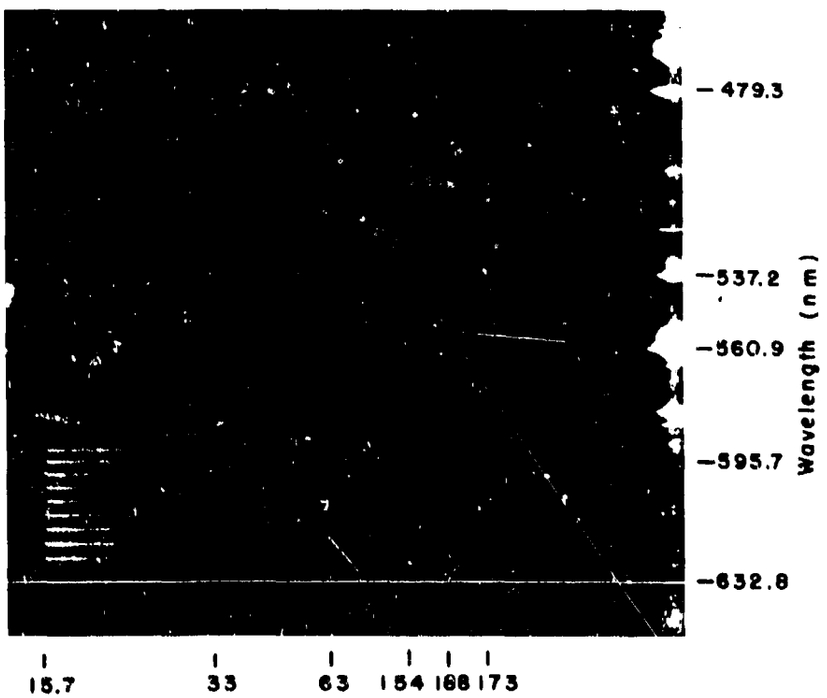

Fig. 5. Light transmission record obtained for GaSe at about 7 K in a two-stage system load coil. Above the diffraction fringes at the bottom of the record are seen several of the exciton absorption bands. The known spectrum of an exploding bridgewire appears at the right of the record.

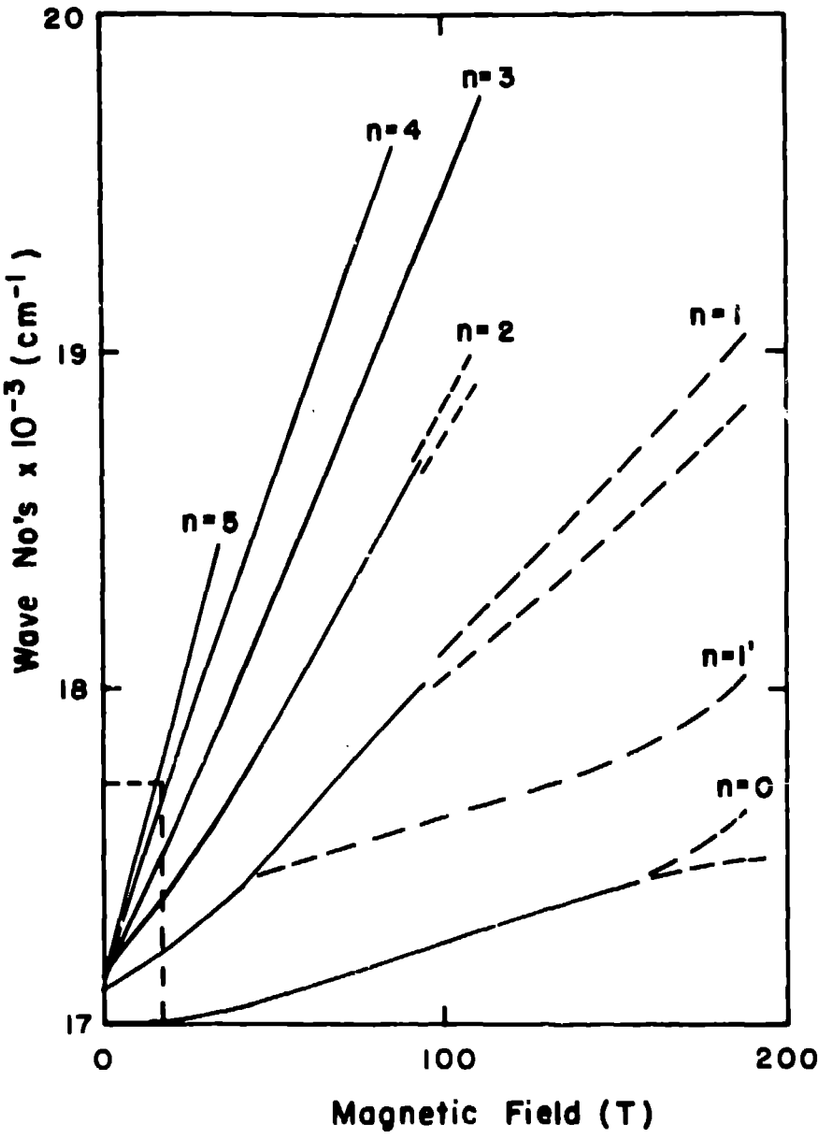

Fig. 6. Tentative exciton level scheme for GaSe at 7 K. The new level n = 1' is weak. The other dashed lines indicate poorly resolved band structure.

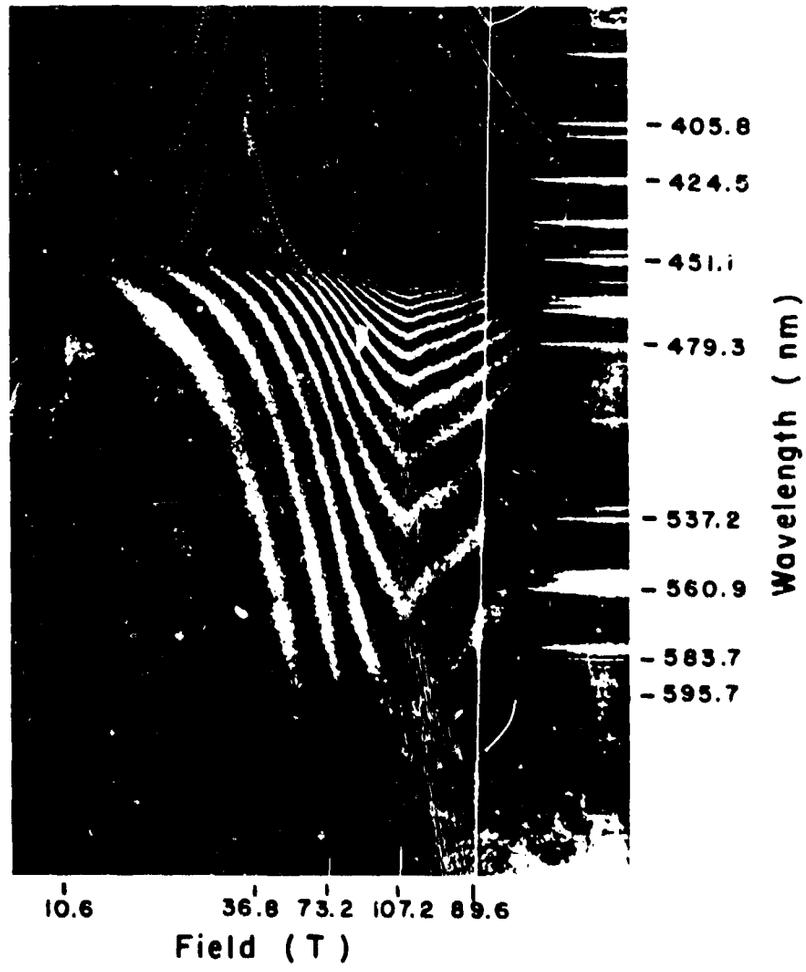

Fig. 7. Faraday rotation record obtained for ZnSe at about 7 K in a single-stage strip system load coil. The absorption edge at about 440 nm is clearly evident.

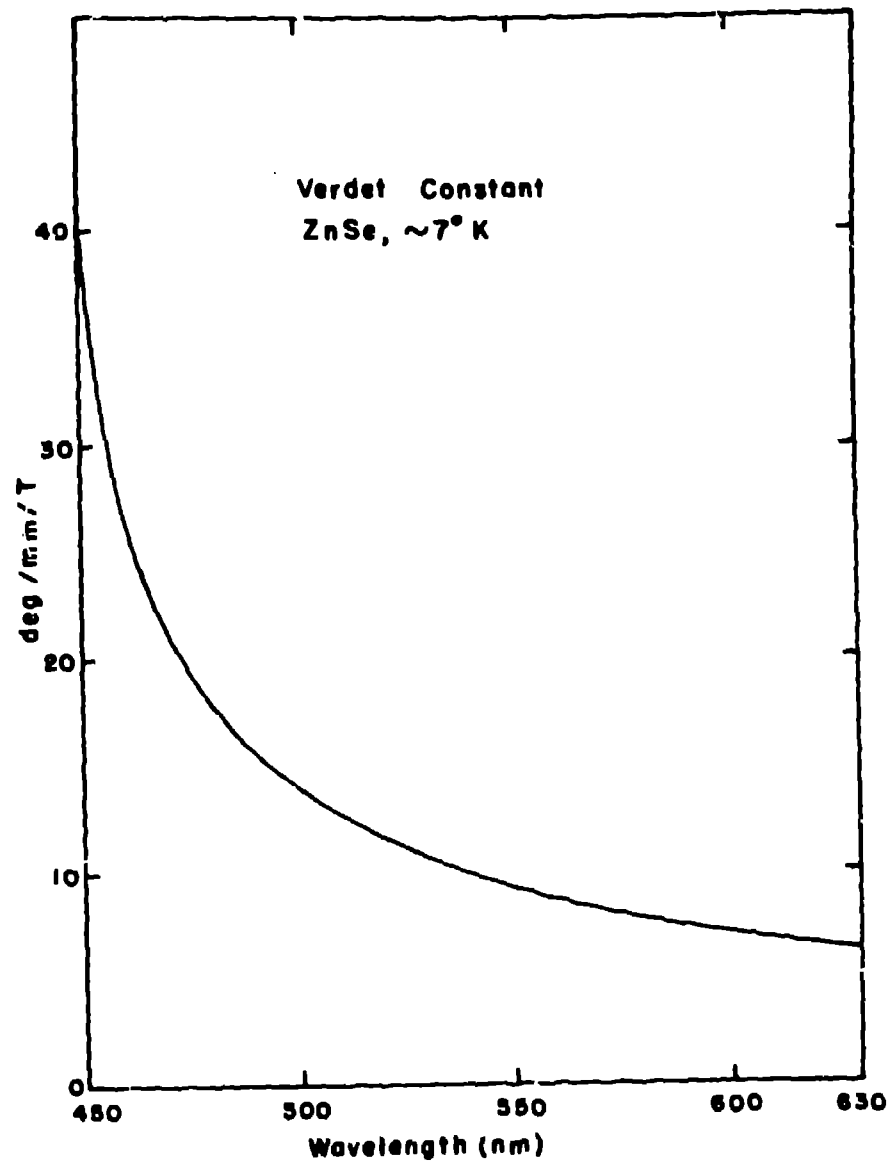

Fig. 8. The Verdet coefficients for ZnSe obtained from the record shown in Fig. 7.

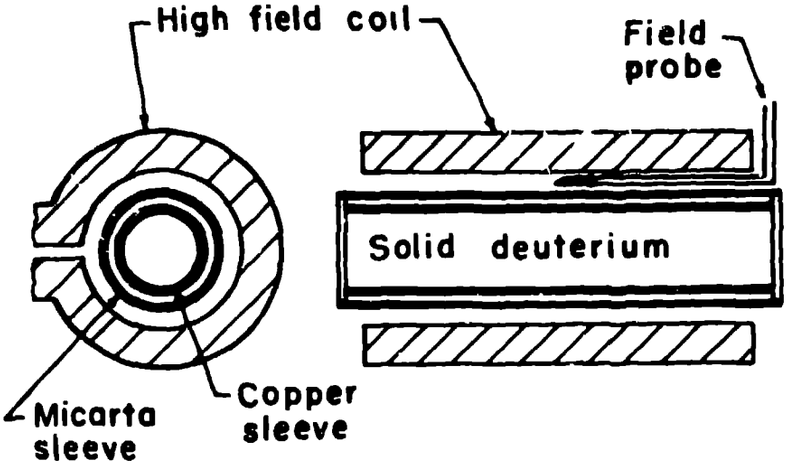

Fig. 9. Schematic drawing of a system used to compress solid deuterium isentropically.

Fig. 10. Flash x-ray radiographs taken for a deuterium compression experiment. The left exposure is a setup shot, while the right exposure was taken during the compression stage when the magnetic drive pressure was 6.5 GPa. The central exposed regions define the effective deuterium sample area. The dark annular rings define spaces between the copper and micarta sleeves and between the micarta sleeve and field coil.